

AFCRC TR 58202

ASTIA Document No. AD 146792

ENGINEERING RESEARCH INSTITUTE
THE UNIVERSITY OF MICHIGAN
ANN ARBOR

Final Report

(In partial fulfillment of the contract)

SOME STUDIES ON A RADIOACTIVE-IONIZATION-GAGE PRESSURE-MEASURING SYSTEM

M. A. El-Moslimany

N. W. Spencer

ERI Project 2406

AIR FORCE CAMBRIDGE RESEARCH CENTER
BEDFORD, MASSACHUSETTS
CONTRACT NO. AF 19(604)-1511

December 1957

Engw

UMR

1307

TABLE OF CONTENTS

	Page
LIST OF FIGURES	iii
ABSTRACT	iv
OBJECTIVE	iv
INTRODUCTION	1
THE RADIOACTIVE IONIZATION GAGE	2
Source Activity Instability	12
Sorption Effects	16
Presence of Impurities	16
Effects of Shape and Strength of Electric Field	18
Temperature Effects	21
CONCLUDING REMARKS	23
APPENDIX. Analytical Investigation of Source Stability	24

LIST OF FIGURES

No.		Page
1	Diagram of NRC Type No. 510 radioactive ionization gage.	3
2	Variation of output current with chamber pressure (room temperature).	5
3	Variation of recombination coefficient α in O_2 as a function of temperature.	6
4	Recombination coefficient α in air as a function of pressure.	7
5	Reduction of recombination loss by using higher collector voltage.	8
6	Change of dark-current value with collector configuration.	10
7	Variation of conduction current with pressure at room temperature for different plate spacing in a planar radioactive ionization gage (constant electrode voltage $V = 50$ v).	11
8	Variation of output current with time.	13
9	Calculated alpha activity of a poorly sealed source.	14
10	Scintillation apparatus.	15
11	Photomultiplier circuit diagram.	17
12	Electric field configuration at an x-section of an NRC No. 510 radioactive ionization gage.	19
13	Variation of conduction current with pressure at room temperature for different electrode voltages in a planar radioactive ionization gage (constant spacing $d = 1/4$ ").	20
14	Change of output current and "gas" temperature with time for various pumping speeds.	22
15	Radioactive transformations of radium and its decay products.	25

ABSTRACT

Radioactive ionization gages are known to exhibit a significant hysteresis effect at gas densities where recombination plays an important role in determining the ionization current. Several possible causes are discussed and have been investigated; results have led to the conclusion that hysteresis is caused by changes in the attachment and recombination coefficients due to gas temperature variations. The report partially fulfills the obligations of the contract.

OBJECTIVE

The purpose of this investigation is to gain a better understanding of the fundamental behavior of a radioactive ionization gage to enable certain improvements of its characteristics to be made.

INTRODUCTION

There has been, for a number of years, a research program in the Electrical Engineering Department of The University of Michigan aimed at determining upper-atmosphere ambient pressures and temperature through the use of sounding rockets. It is part of the upper-atmosphere research program of the Air Force Cambridge Research Center, Geophysics Research Directorate, and has enjoyed sponsorship by that organization.

The research has been concerned chiefly with measurements at altitudes above those readily attainable with balloons, and thus has been concentrating on the development of techniques and instruments that can perform creditably in a high-velocity rocket.

In the general measurement plan, air pressures are measured at selected points on the surface of the rocket nose cone from which measurements of the flow Mach number may be determined. Subsequent interpretation of the Mach number with knowledge of the rocket trajectory combined with certain reasonable assumptions permits calculation of ambient air temperature.

The pressure measurements forming the basis for the temperature determinations have been accomplished through use of radioactive ionization gages. Although several types of gages can be employed over portions or all of the pressure range concerned, it is the belief of The University of Michigan group that the radioactive ionization gage is best suited for many reasons, including the following:

- 1) It is physically rugged.
- 2) It responds adequately over the desired pressure range.
- 3) It can be operated without damage at atmospheric pressures.
- 4) It responds without delay to density change.
- 5) Its current-density characteristic is linear over a considerable range.

However, it has certain drawbacks:

- 1) The presence of the radioactive source constitutes a potential health hazard.
- 2) The signal level is quite low, requiring appreciable electronic circuitry.
- 3) In certain portions of the operating range, the output current appears not entirely dependent on the gas density, apparently exhibiting a tangible variation (hysteresis) for unknown reasons.

The circuitry developed for use with the gage employs high resistances, a negative feedback amplifier, and self-induced range changing, which allows the intended total range of several pressure decades to be resolved in terms of several sub-ranges, without outside control, during a rocket flight.

A total of from 15 to 20 radioactive ionization gage systems have been employed on several Aerobee rocket flights which have demonstrated that the equipments have merit for this service. The data produced have proven reliable, except for pressures above about 10 mb, a limit imposed by an unsuitable or misunderstood gage characteristic.

The objectives of the research reported on here are to improve the radioactive ionization gage system by (1) investigating the fundamental characteristics of the radioactive ionization gage to eliminate the undesirable effect (hysteresis), as well as generally to improve response and linearity of the gage characteristic, and (2) redesigning the associated electronic system to reduce weight, volume, power consumption, and operating complexity. Neither of these objectives was entirely satisfied by the effort expended under this particular contract. The work was continued, however, in a broader effort including the carrying out of upper-atmosphere measurements. The later effort, still in progress at the time of writing, has resulted in the design of a chamber that reduces the hysteresis effect to a nearly negligible amount, and provides a sensitivity adequate for the measurement to pressures at least as low as 10^{-3} mb. The associated circuitry has likewise been redesigned to meet the desired objectives. A discussion of details of these equipments is necessarily confined to the report on the contract covering that work, AF 19(604)-1948.

THE RADIOACTIVE IONIZATION GAGE

Before discussing investigation of the characteristics of the radioactive ionization gage chamber, a brief account of the gross aspects of the operation of the device may be useful.

A radioactive ionization gage is a gage in which the ionization is produced by the impact of high-energy particles from a radioactive source, usually radium, upon gas particles. A typical chamber, illustrated in Fig. 1 (National Research Type No. 510), is provided with a collector (C), a polarizing electrode (A), and a radium source (B).

The radioactive source consists of a small plaque, on one side of which is the active area, a radium-gold alloy. To increase the efficiency of the source as an alpha emitter, the plaque is electroplated with nickel. The nickel film acts as a seal and thus enables retention of radon gas and its decay products which yield three more alphas for every alpha particle produced by the radium. A d-c field is established between the collector (C) and electrode (A)

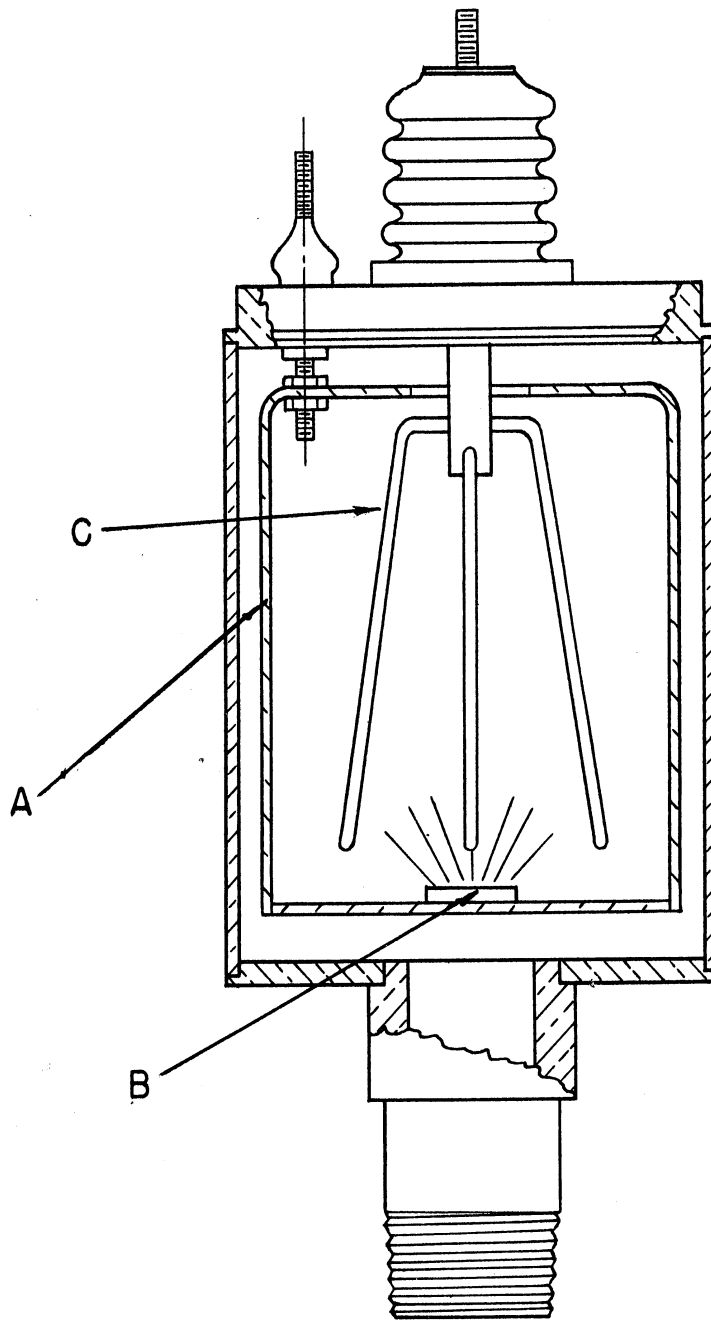


Fig. 1. Diagram of NRC Type No. 510 radioactive ionization gage. (A) electrode, (B) radium source, (C) collector electrode.

to effect collection of the products of ionization which include positive ions, electrons, and negative ions. Ionization produced by alpha particles from this type of source is essentially anisotropic due to the high energy (about 5 mev) of the alphas; thus the process is generally referred to as columnar ionization. The number of collected ions depends on the density and hence on the pressure of the gas in the chamber, provided that the temperature is held constant and the field is strong enough to collect all products of ionization. This is known as the saturation ion current and can be expressed in the simple form, $i = \text{constant} \times \text{pressure}$. Hence the value of the ion current may be taken as a measure of pressure. The gage has a nonlinear i - p curve in the high- as well as in the very low-pressure regions as shown in Fig. 2, a typical characteristic of NRC gage type No. 510.

The departure from linearity at the upper end of the pressure range is mainly due to ion recombination, corresponding to relatively low values of field to pressure ratio. The type of recombination taking place is predominantly columnar, with some likelihood of volume recombination due to the diffusion of ions into the chamber space shortly after their generation. The rate of recombination at any point is given by

$$i_c = \frac{dq_c}{dt} = \alpha n^- n^+ = \alpha n^2 ,$$

where $n^- \approx n^+ = n$ are the negative and positive ions, respectively, and α is the recombination coefficient, temperature- as well as pressure-dependent, as illustrated in Figs. 3 and 4.

Ion production is linearly related to the gas density, whereas the loss of ions by recombination is proportional to the square of the gas density. These concepts and the fact that the recombination coefficient increases with pressure in the range of from 5-1200 mb, satisfactorily explain the departure from linearity in the upper portion of the pressure range, provided each alpha still possesses a modest fraction of its original energy when it reaches the wall of the chamber.

The concept of recombination before collection can be confirmed by noting that it is possible to extend the linear portion and thus almost eliminate the nonlinearity at the upper end of the pressure range simply by increasing the intensity of the polarizing field. In this case almost all ions produced are collected, rather than experiencing ion-ion recombination as illustrated in Fig. 5.

On the other hand, at the lower portion of the pressure range, below 10^{-2} mb, nonlinearity of the i - p characteristic cannot be attributed to recombination, since the gas density and the value of the recombination coefficient are relatively very small at these densities. Study of the i - p characteristic at the low pressures reveals that this part of the curve is the sum of at least two currents. One is the expected linear variation of current proportional to

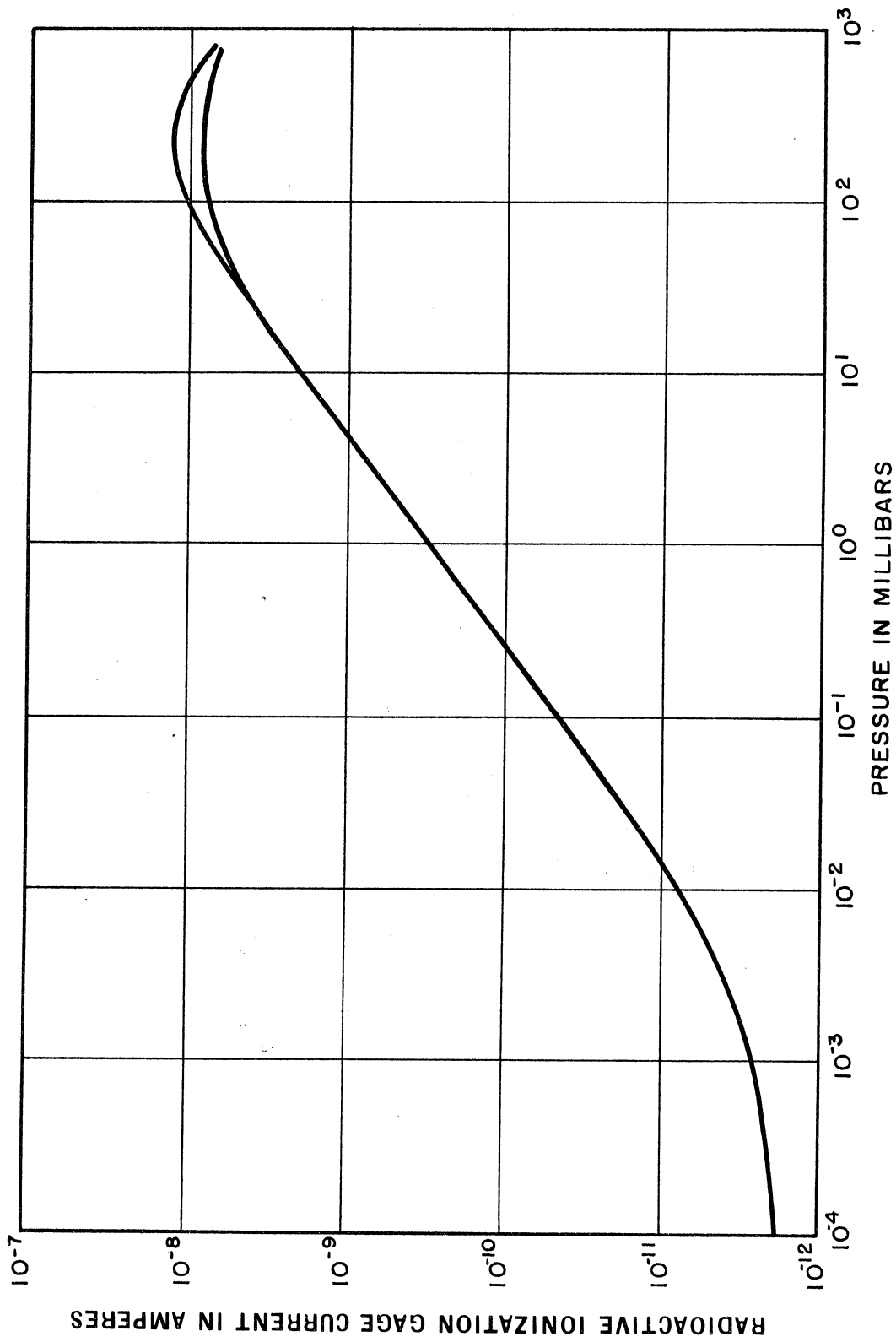


Fig. 2. Variation of output current with chamber pressure (room temperature).

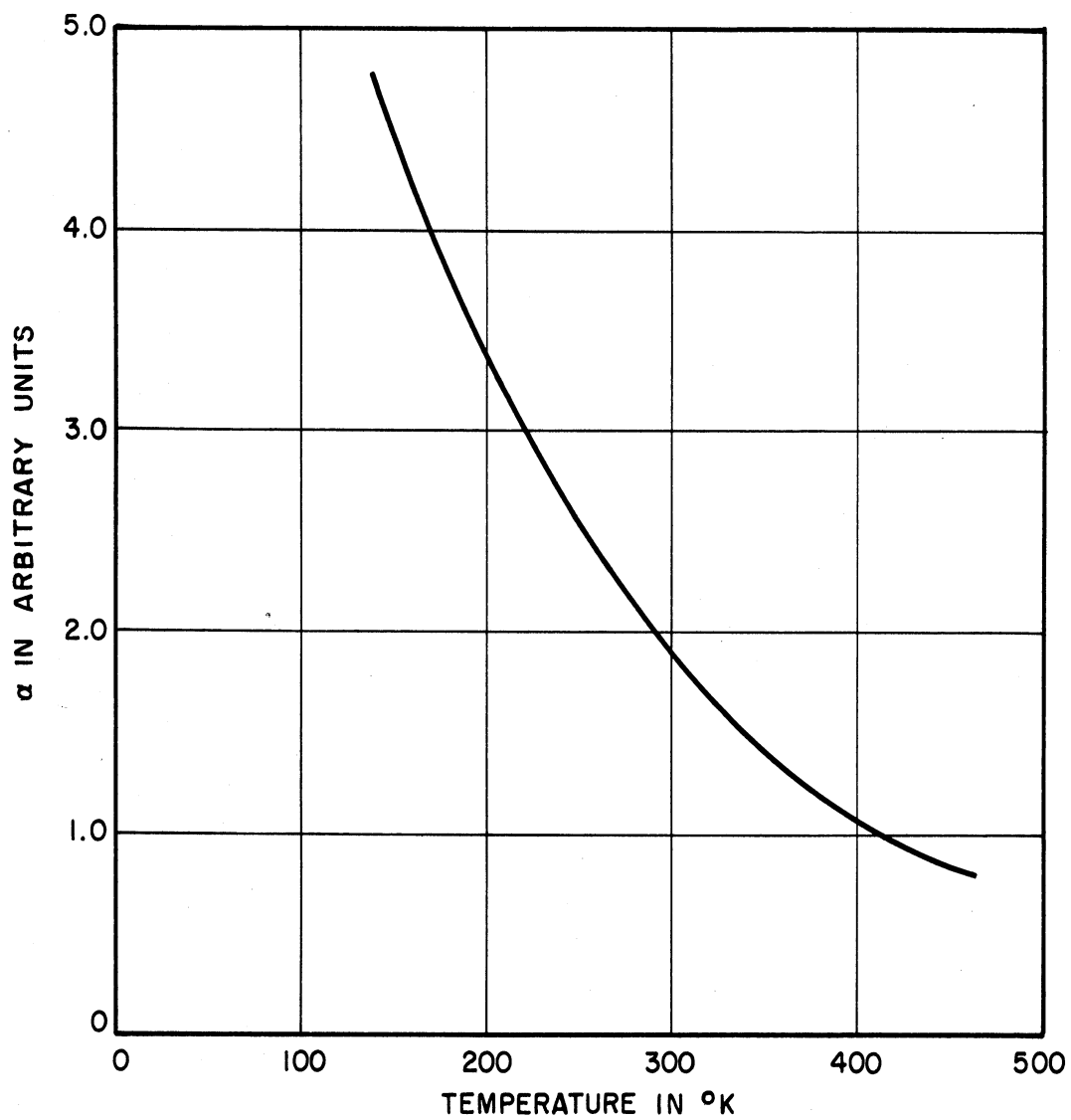


Fig. 3. Variation of recombination coefficient α in O_2 as a function of temperature.

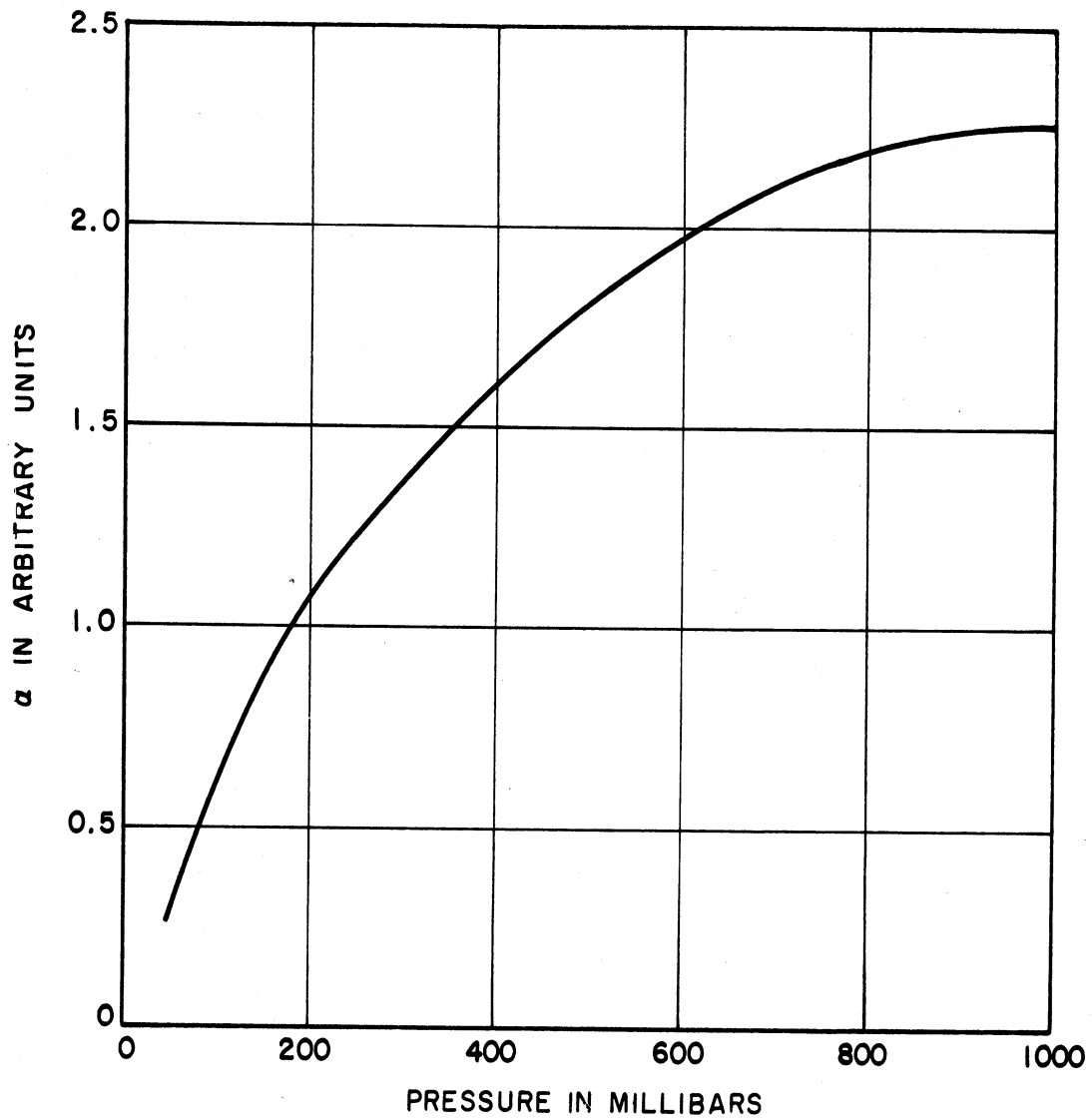


Fig. 4. Recombination coefficient α in air as a function of pressure.

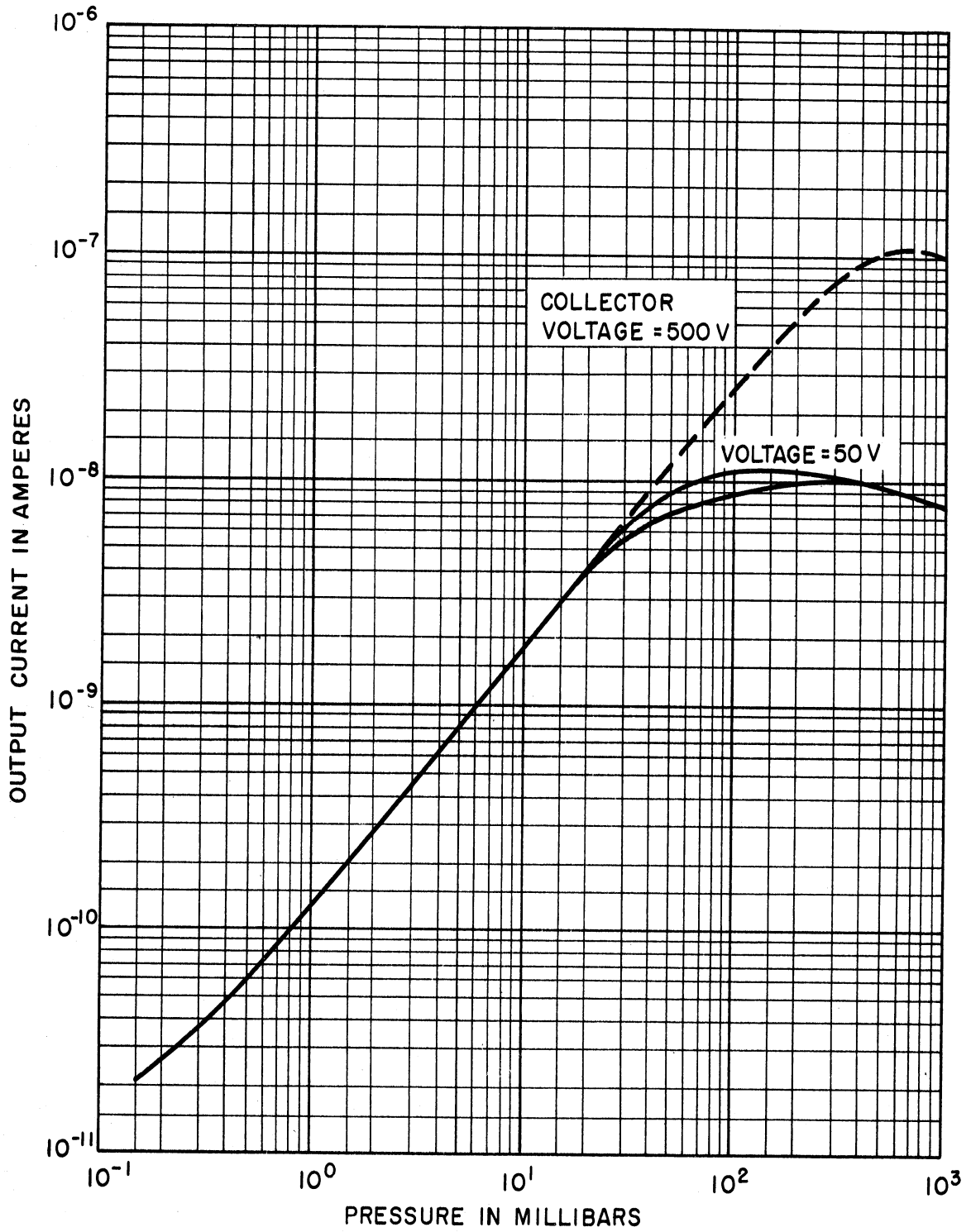


Fig. 5. Reduction of recombination loss by using higher collector voltage.

gas density and the other is essentially a constant which has been termed the "dark current" of the gage.

The dark current was found to depend upon (a) the strength of the source used as an alpha emitter, (b) its orientation inside the ionization chamber, and (c) the configuration of this chamber. In general, the greater the number of alpha particles reaching the positive-ion collector, the greater is the magnitude of the resulting dark current. It is thus possible to lower the value of the dark current and consequently extend the linear portion of the i-p characteristic to lower pressures by reducing in some manner the number of direct impacts of alphas on the collector. This is illustrated in Fig. 6 which shows the i-p characteristics of two radioactive ionization gages, identical in every respect except for the configuration of the position-ion collector which is a plane disc in one case and a thin wire in the other.

The secondary electrons emitted as a result of the impacts of the high-energy alpha particles on the collector surface also contribute to the constant current. This contribution is primarily dependent upon the number and energy of impinging particles, which undergo no appreciable change under pressures lower than about 10^{-2} mb.

Figure 7 shows the i-p characteristics of one planar radioactive ionization gage for different plate spacings. The curves appear to converge into a single line, suggesting that the dark current results from the secondary-emission effects and the collection of the alpha particles whose number is practically invariant in this particular configuration for the different spacings indicated in the figure.*

In addition to the nonlinearity, the radioactive ionization gage exhibits another and less desirable phenomenon: if one observes the current, when, for example, the pressure is permitted to decrease from atmospheric to some arbitrary value and then to increase to the original pressure, the two current-pressure curves observed do not coincide. This deviation occurs mainly in the high-pressure nonlinear portion as shown in Figs. 2 and 5.

Hysteresis in the upper range of pressure was believed possibly due to one or more of the following factors:

1. Variation in source activity.
2. Gas sorption, (possibly selective) by the inner surfaces of the ionization chamber.
3. Effects due to contamination in the presence of water vapor.
4. Recombination effects.
5. Effects of shape and strength of electric field.
6. Temperature effects.
7. Other unknown effects.

*Later investigation showed that x-ray emission from the chamber walls due to impacts of alphas causes appreciable electron emission from the collector.

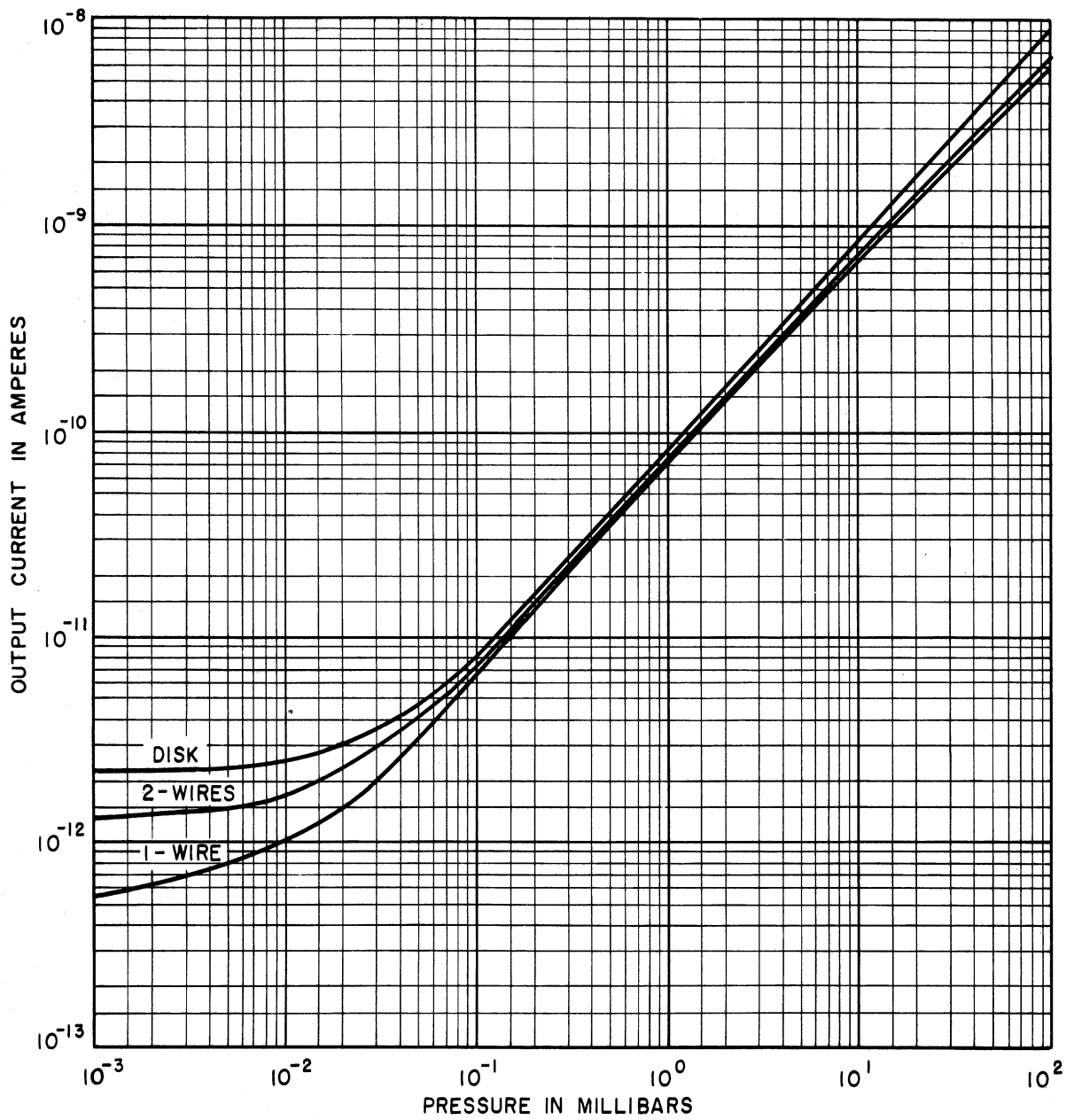


Fig. 6. Change of dark-current value with collector configuration.

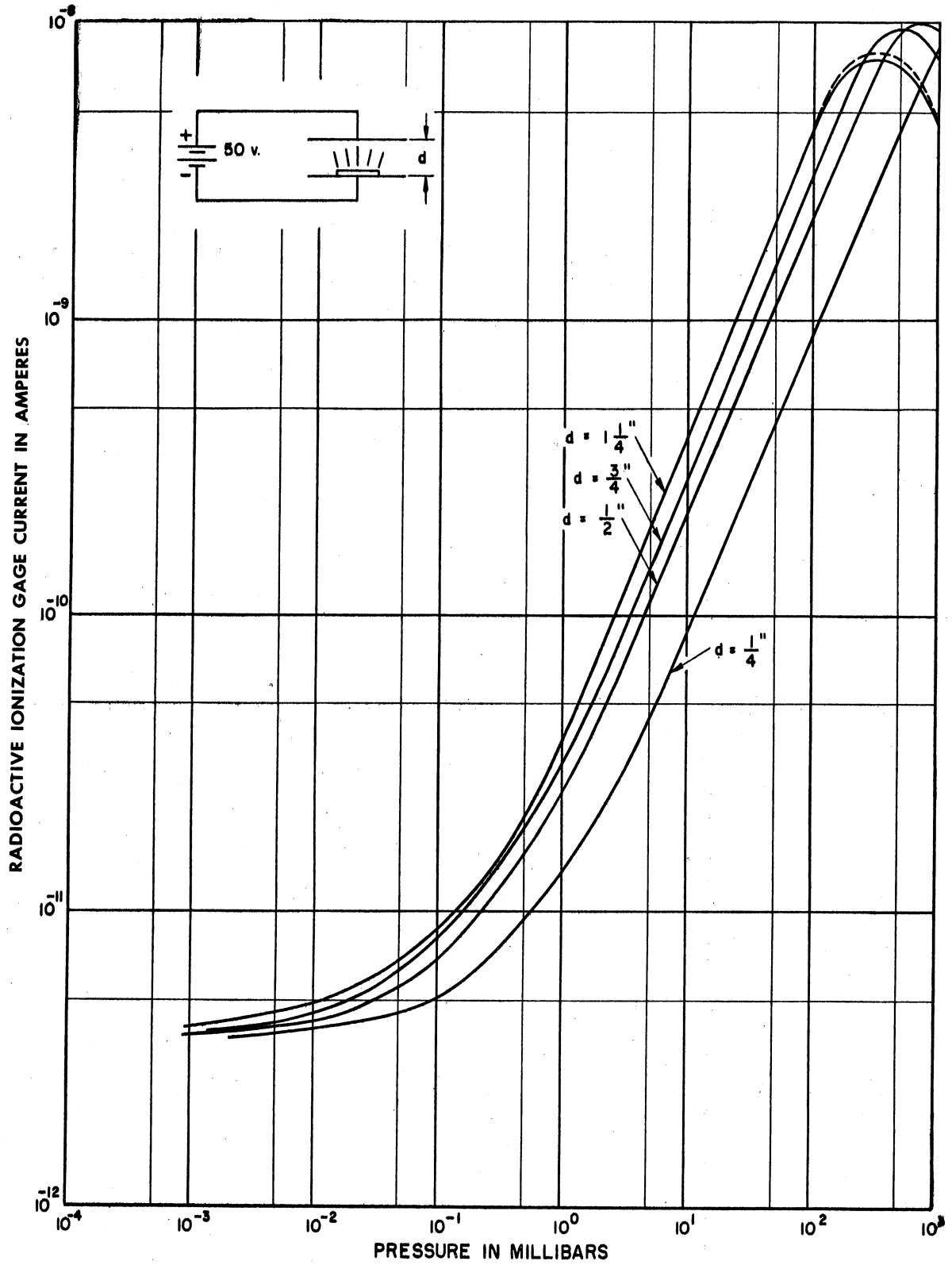


Fig. 7. Variation of conduction current with pressure at room temperature for different plate spacing in a planar radioactive ionization gage (constant electrode voltage $V = 50$ v).

For better observation of hysteresis, the following procedure was adopted. The pressure inside the gage was maintained at about 10^{-4} mb for about 72 hours and was then abruptly increased to atmospheric pressure ≈ 1000 mb. Concurrently the collected current was observed until it attained a steady value. This procedure was repeated for different final pressures, lower than atmospheric. Typical results of this experiment are shown in Fig. 8. From these curves we notice that the current first decreases until it reaches a minimum after about one hour, and then increases to reach a final value slightly higher than the minimum. It was also noticed that the greatest dip in current occurs at a pressure roughly equivalent to the pressure at which the peak occurs.

SOURCE ACTIVITY INSTABILITY

These results first suggested instability of source activity, that is, lack of equilibrium between the radium and its daughter products through loss of radon by leakage through the seal. Accordingly, a mathematical analysis of the source strength as an alpha emitter was developed, taking into account the various levels of alpha particle energy involved (see the Appendix). Although the general shape of the calculated curves obtained, shown in Fig. 9, is somewhat similar to the experimental ones, the relative dip in the curves is comparatively much smaller and sometimes even negligible, indicating relative constancy of source activity.

To verify this result experimentally, a scintillation apparatus was assembled. A sketch of the source and phototube portion of the device is shown in Fig. 10. The radium source was mounted on a monel frame inside a glass tube facing a mica window which served as a vacuum-tight seal, while being sufficiently transparent for most alpha particles to pass. The external side of the mica seal faced the window of a DuMont 6467 photomultiplier.

An appropriate layer of ZnS:Ag phosphor (about 8 mg/cm^2) was deposited on the outer surface of the photocathode according to the following procedure. The activated zinc sulfide powder was dispersed in distilled water and poured into a settling chamber made from a piece of glass tubing fitted over the end of the photomultiplier with a rubber gasket to prevent leakage. Suitable amounts of barium acetate and potassium silicate were also added to give an evenly dispersed and highly adherent film. The phosphor was allowed to settle; then most of the water and unused potassium silicate solution were slowly removed with a pipette, and the remainder was permitted to evaporate into the atmosphere.

The minimum practical distance between the source and the phosphor film was determined by two desires: (a) to protect the phosphor film from destruction by the high-energy-particle bombardment, and (b) to minimize dispersion of the alpha particles.

The glass tube and the photomultiplier were enclosed in a light-tight mag-

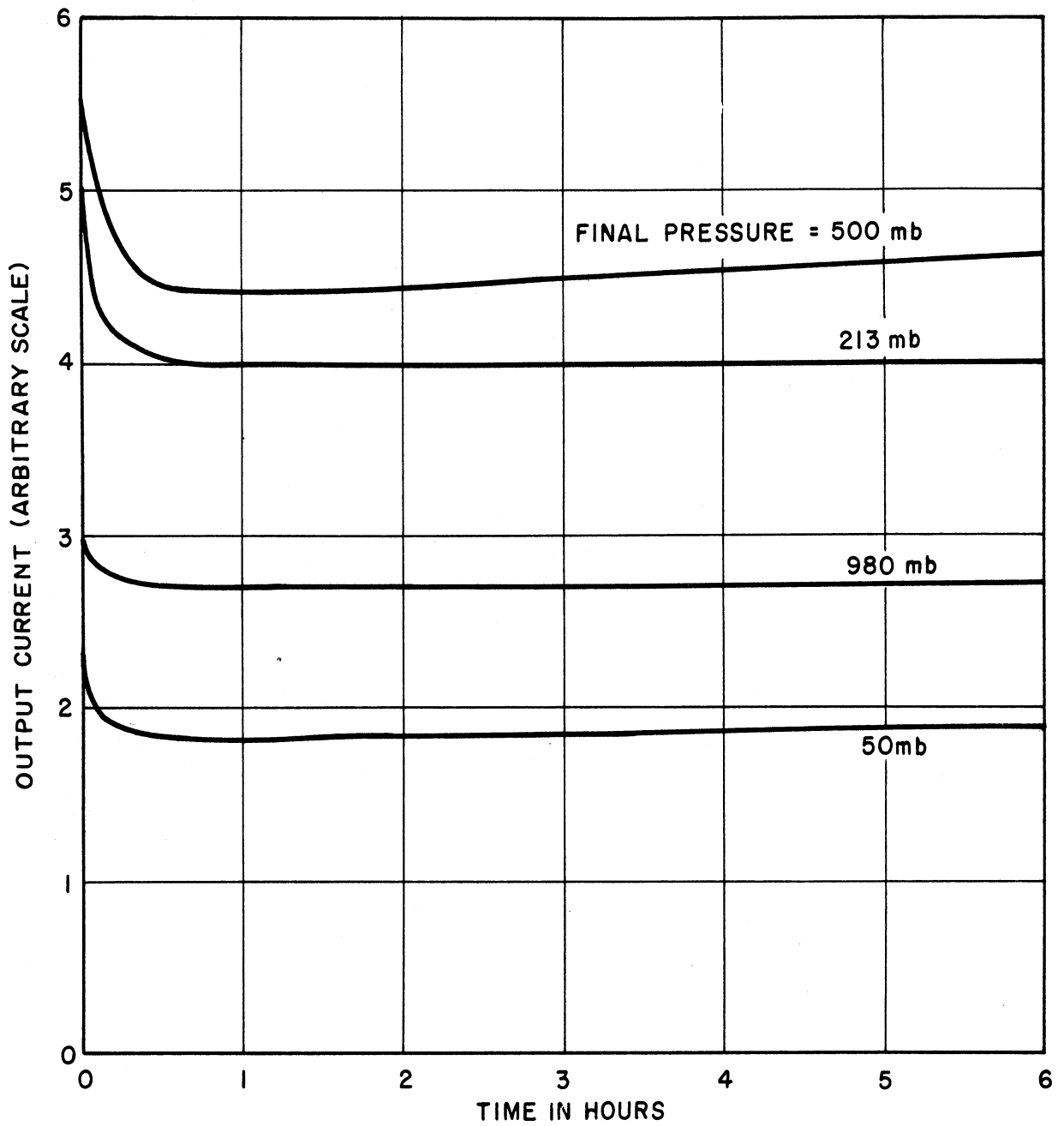


Fig. 8. Variation of output current with time.

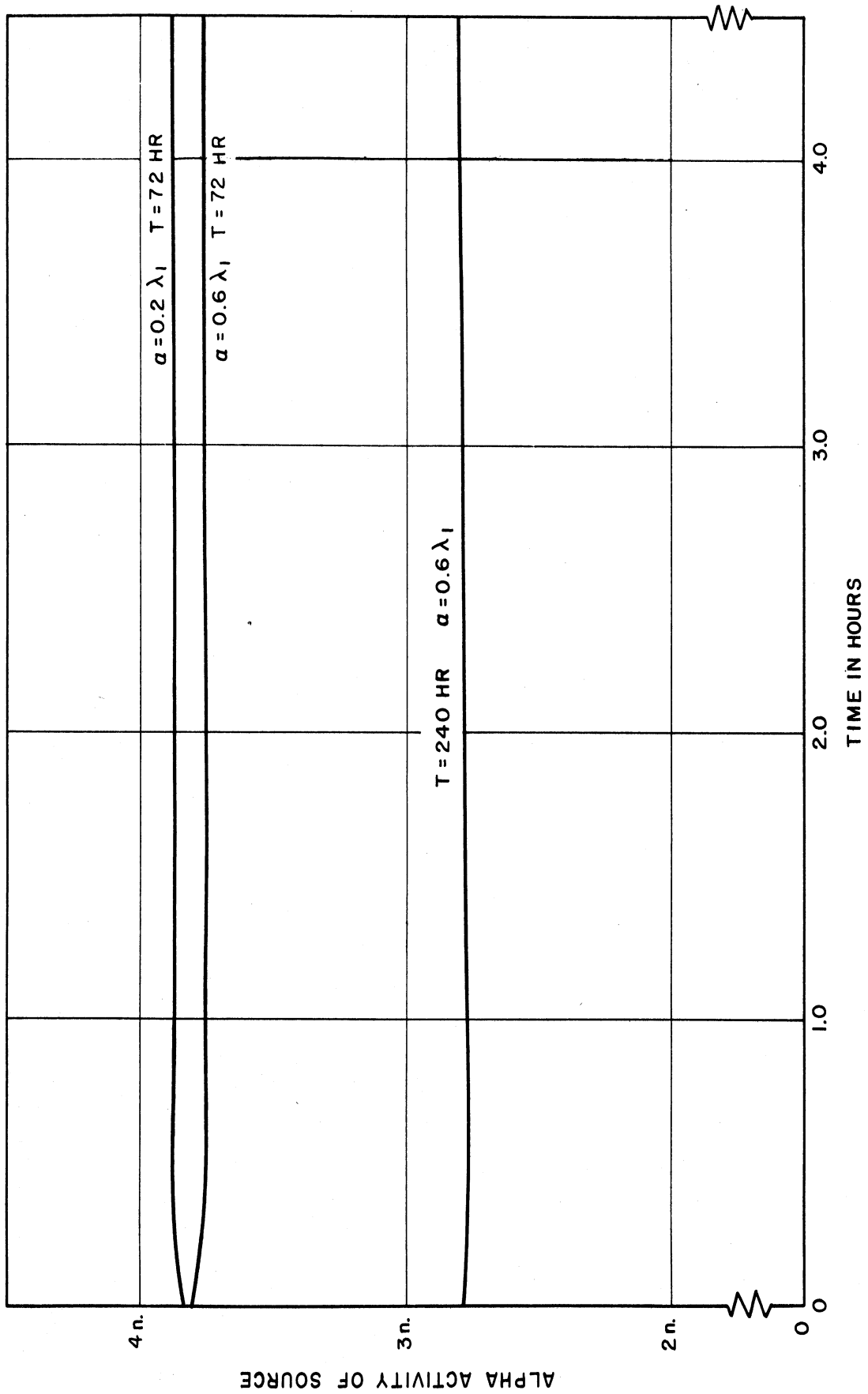
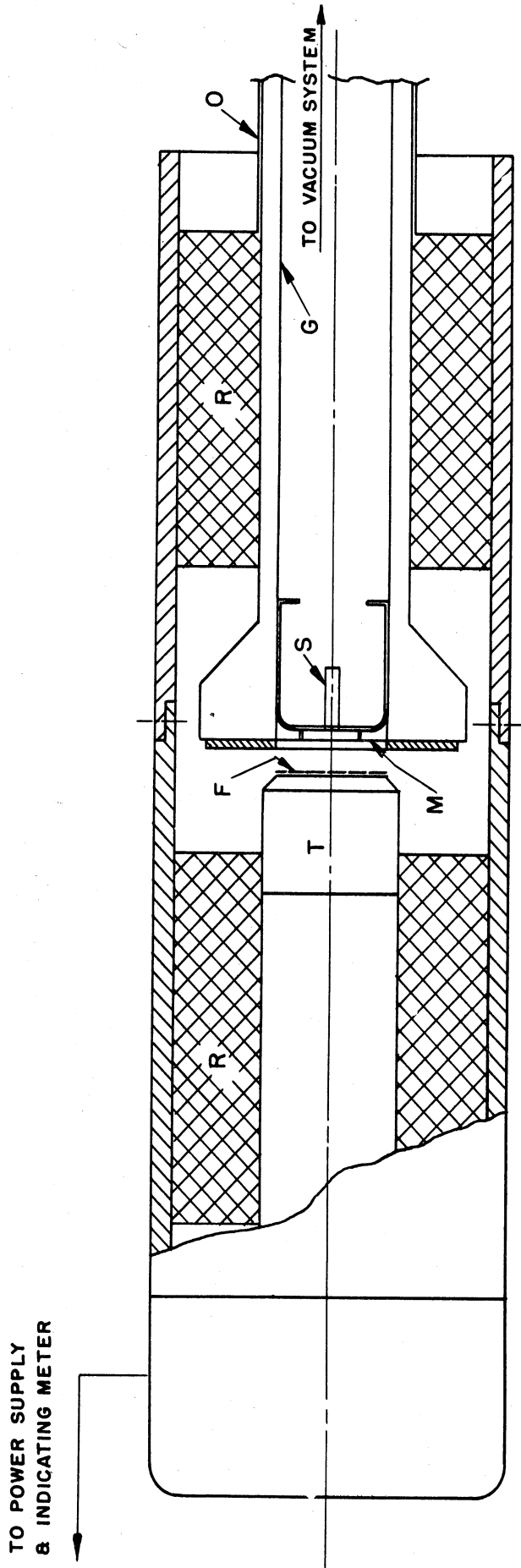


Fig. 9. Calculated alpha activity of a poorly sealed source.



- S - RADIOACTIVE SOURCE
- M - MICA WINDOW (2.0mg/cm²)
- F - PHOSPHOR FILM (8.0mg/cm²)
- T - PHOTOMULTIPLIER (DU MONT 6467)
- G - GLASS TUBING
- R - BLACK FOAM RUBBER
- O - OPAQUE COATING

Fig. 10. Scintillation apparatus.

netic shield. The required voltages at the phototube dynodes were so adjusted that the average anode output current was limited to about 50 μ a, a value which is far below the maximum rating of the tube. This low value is advisable to assure adequate stability conditions for operation of the phototube as far as secondary-emission current is concerned. These voltages were supplied by a convenient power supply, illustrated in Fig. 11, from which voltages up to 2400 volts were available.

Owing to the fluorescent property of ZnS:Ag material, some of the energy absorbed from the alpha particles is re-emitted as light (scintillations) quantitatively proportional to the energy lost by the incident radiation, i.e., proportional to the incident number of particles.

The apparatus was connected to the vacuum system to enable observation of possible variation of activity with pressure. The system was first pumped out to 10^{-3} mb where it was maintained for about 48 hours, after which air was admitted to bring the pressure abruptly to atmospheric, where it was maintained for about 6 hours. Throughout this procedure no appreciable change in the output current was observed. The test was repeated several times with longer periods under vacuum, giving the same constant output value.

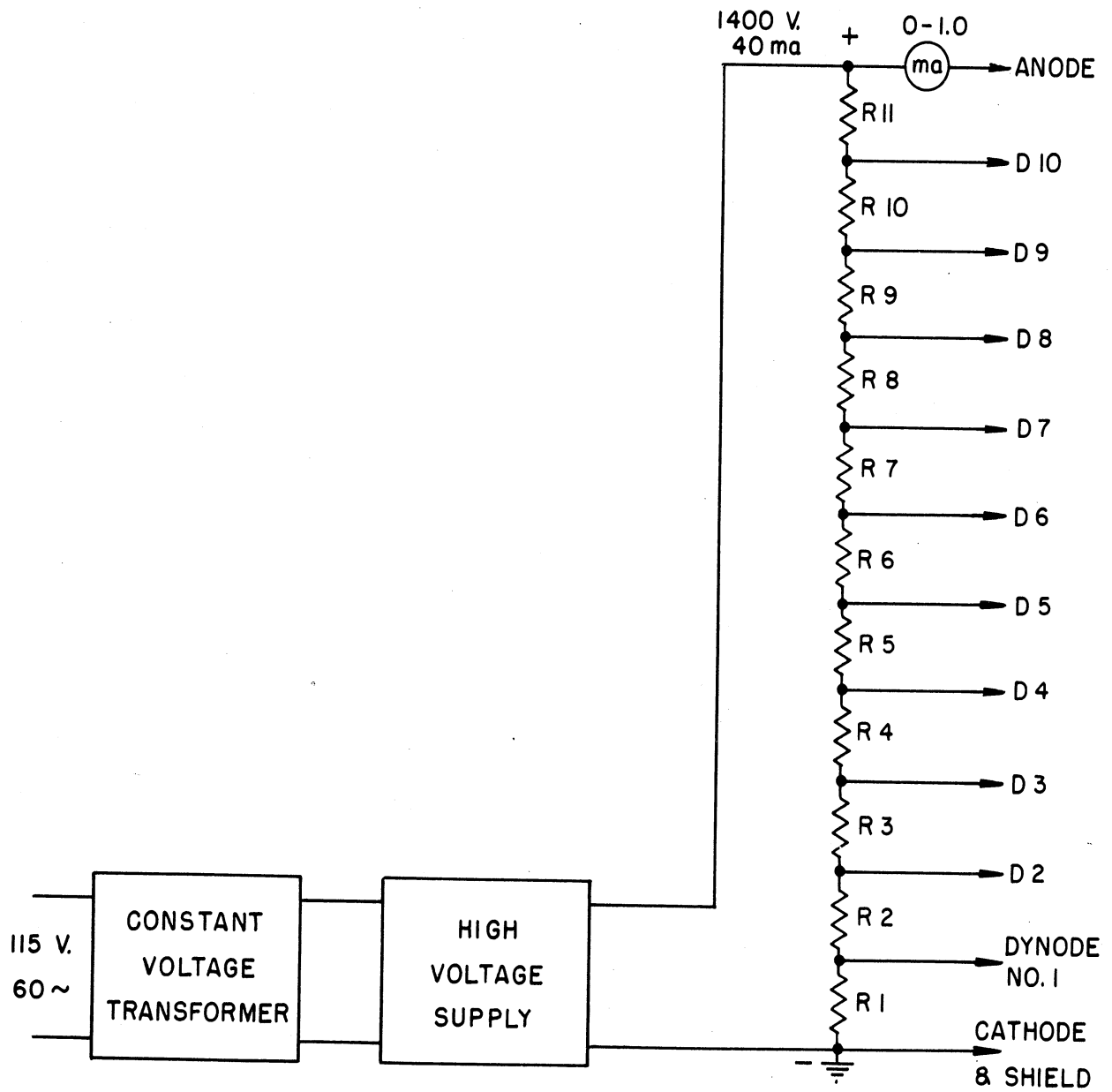
This result was interpreted as indicating constancy of source strength, and it was accordingly concluded that the variation of the collected ionization current at a given pressure was not due to a change of source strength.

SORPTION EFFECTS

Differing wall affinity for gases from one gas to another suggested the possibility of selective adsorption in gas mixtures such as air. To observe the effect of such selective adsorption on the reproducibility in the i-p relation of the radioactive ionization gage, readily available tank nitrogen was used instead of the room air. After flushing the system several times so as to assure a reasonably clean nitrogen atmosphere, the i-p characteristics were again taken for this monogas radioactive ionization gage. Since these curves showed the same magnitude of hysteresis as experienced in the case of room air, it was concluded that selective adsorption of some constituents of an air mixture is not responsible for this hysteresis. In arriving at this conclusion, it was recognized that ideal purity conditions were not achieved and it was thus likely that only gross effects were observed.

PRESENCE OF IMPURITIES

A new and smaller gage was constructed of glass and carefully cleaned to afford surfaces reasonably free of oxides or contaminating chemical compounds. A new, presumably clean, radium source was used in this gage. Using the same nitrogen as before, tests revealed hysteresis as experienced with the original



R1 - 6000 ohms, 20 watts

R2 - R11 - 3000 ohms, 10 watts

Fig. 11. Photomultiplier circuit diagram.

gage. Special consideration was given to water vapor. In this regard, Bortner and Hurst have found that the presence of water vapor apparently has a negligible effect on the gage sensitivity.*

EFFECTS OF SHAPE AND STRENGTH OF ELECTRIC FIELD

Consideration of the distribution of the electric field inside the NRC radioactive ionization gage led to the following conclusions. The field is quite nonuniform; there is high intensity in the vicinity of the ionization-chamber walls, as contrasted with the bulk of the ionization chamber which is in a region of considerably lower intensity (Fig. 12). Because of this weak field pocket (inside the dotted circle, Fig. 12), saturation could hardly be attained and any slight changes in electric field could have a tangible effect on the collected ion current.

The voltage applied to the electrodes in this gage type is usually between 30 and 50. Applying a much higher value (500 v, for example) to the electrodes, the field is still nonuniform but much more intense. It was thus possible to extend the linearity up to 400 mb, i.e., ten times the normal range. Thus, over a pressure range where at low field strengths the hysteresis phenomenon prevailed, the i-p relation is made linear, and the hysteresis effect is apparently eliminated. However, hysteresis is now observed at higher pressures in the newly located "hump" region (600-1000 mb).

To simplify the field shape and to obtain an essentially uniform field, a planar radioactive ionization gage was made for our study. This consisted of two parallel two-inch-square copper plates arranged so that the spacing could be adjusted to any value between 1/4 and 1-1/2 in., in 1/4-in. steps. A radium source (approximately 1 mg) was mounted on one of the plates so that it could be directly connected or insulated from that plate. Provisions for reversing plate polarities were also made to permit study of the behavior of the collected ion current when the source was located at either the collector or the electrode side.

In the first set of tests, the source was part of the collector and the spacing between the plates was kept constant at 1/4 in. The field intensity between the plates was varied.

The tests on this planar radioactive ionization gage were carried out for each voltage in the same way as in previous experiments by cyclically pumping out and admitting air at appropriate intervals so that the relations, shown by Fig. 13, could be obtained.

It has been observed, as a result of this series of tests, that the i-p characteristic for this gage configuration was independent of field strength

*Bortner, T. E., and Hurst, G. S., "Ionization of Pure Gases and Mixtures of Gases by 5-mev Alpha Particles," Phys. Rev., 93, 1236-41 (March, 1954).

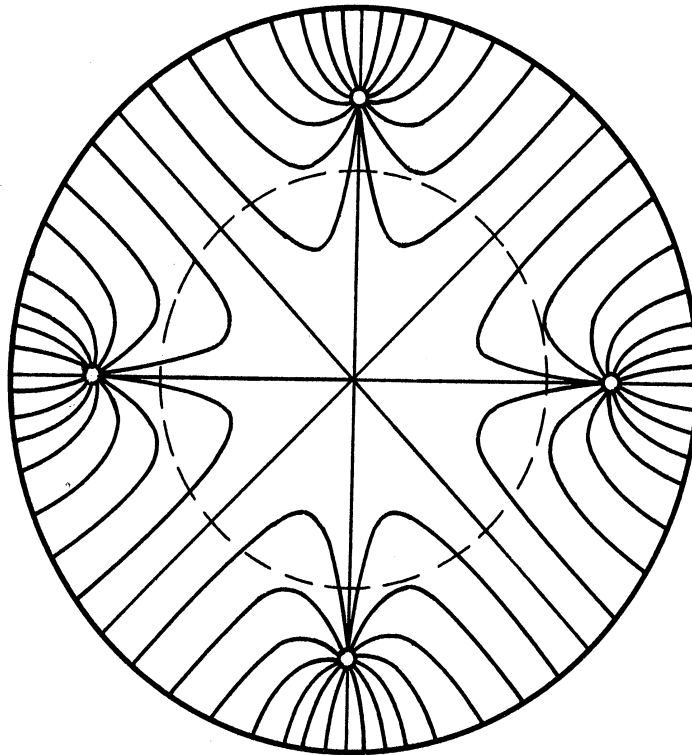


Fig. 12. Electric field configuration at an x-section of an NRC No. 510 radioactive ionization gage.

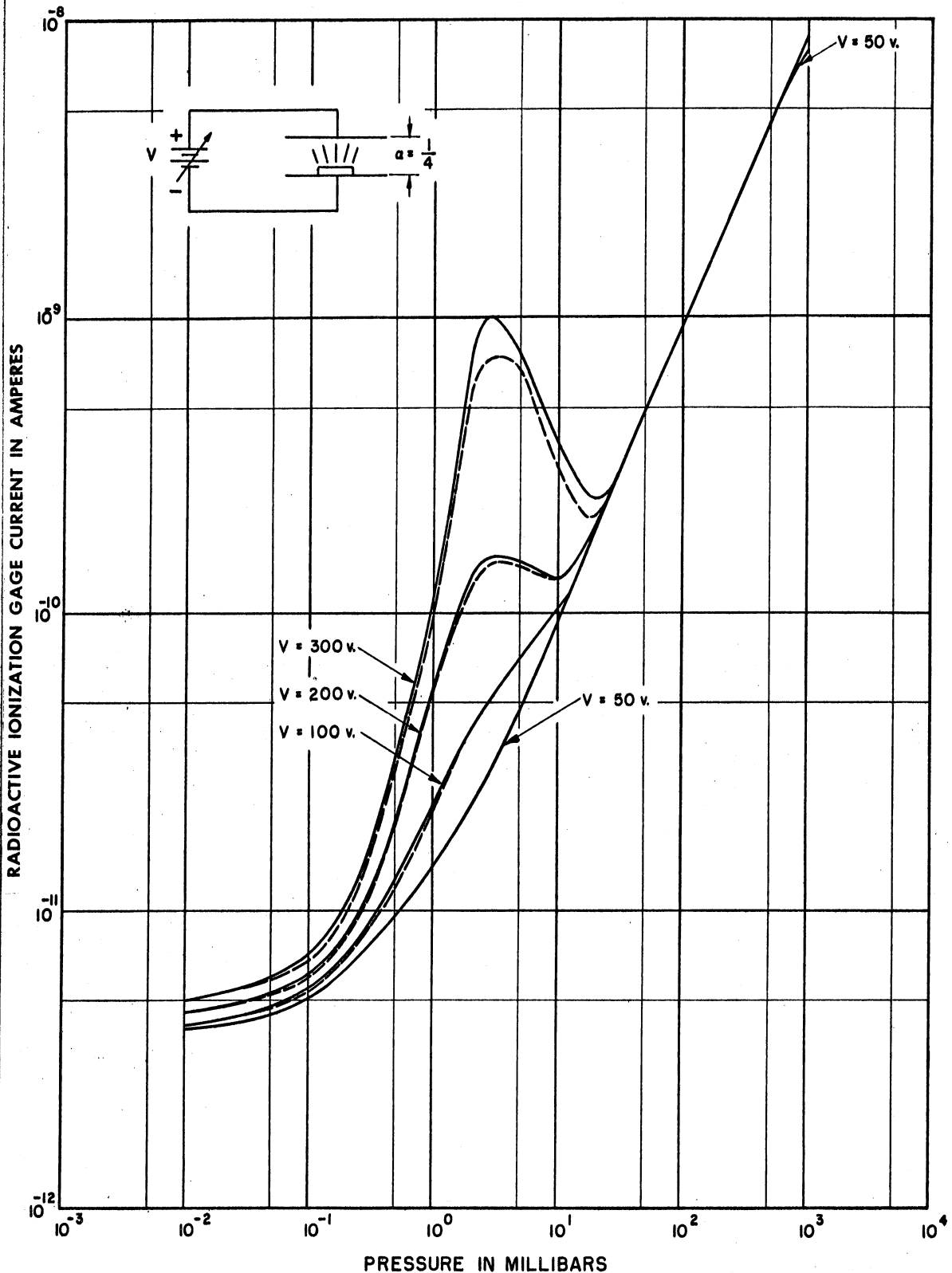


Fig. 13. Variation of conduction current with pressure at room temperature for different electrode voltages in a planar radioactive ionization gage (constant spacing $d = 1/4$ ").

in the region 30-700 mb, where, because the relation is linear, it is presumed that the current is at its saturation value. At pressures less than 30 mb, the characteristic began to show an increase in the collected current for continued pressure decrease as a result of gas amplification, passing through a maximum at approximately 3 mb, below which the current again decreased, becoming asymptotic to about 4×10^{-12} amperes.

At pressures higher than 700 mb, the relation was still linear for electrode voltages of 300, 200, and 100, while it showed a slight deviation from linearity as the electrode voltage was reduced to 50.

In the second set of experiments, the electrode voltage was maintained constant at 50 while the spacing between the plates was varied in 1/4-in. steps. The increase in spacing is equivalent to increasing the volume of the ionization chamber and, hence, the number of ion-pairs generated. Figure 7 shows the predictable proportional upward shifts in the i-p characteristics according to redoubling of plate spacing.

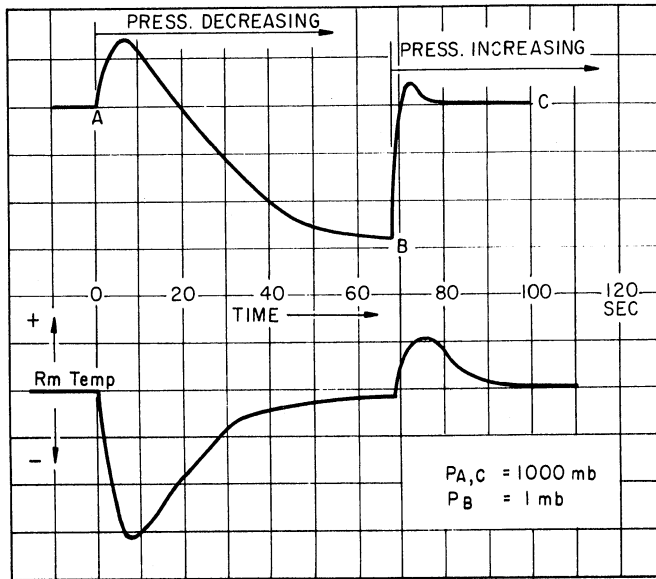
Any increase in spacing gives rise to the production of more ions on the one hand and a reduction in field strength on the other, provided the electrode voltage remains constant. Accordingly, the recombination effect predominates in the upper region to the extent that the collected ion-current is effectively reduced, showing the humps previously observed in the NRC No. 510 radioactive ionization gage.

It was noted that as the effective field between the plates is decreased, the gage starts to show some hysteresis, the magnitude of which increases with further reductions in the field intensity.

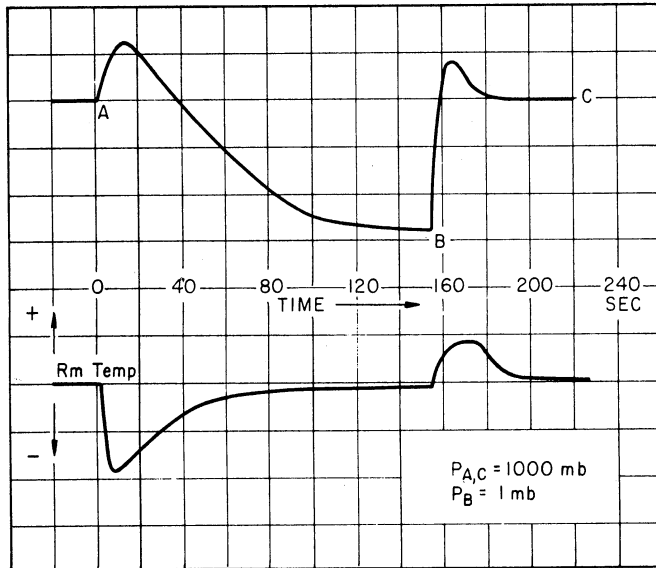
The previous observations suggest that, under high ion concentration in comparatively weak fields and the presence of weak field pockets, hysteresis is likely to occur.

TEMPERATURE EFFECTS

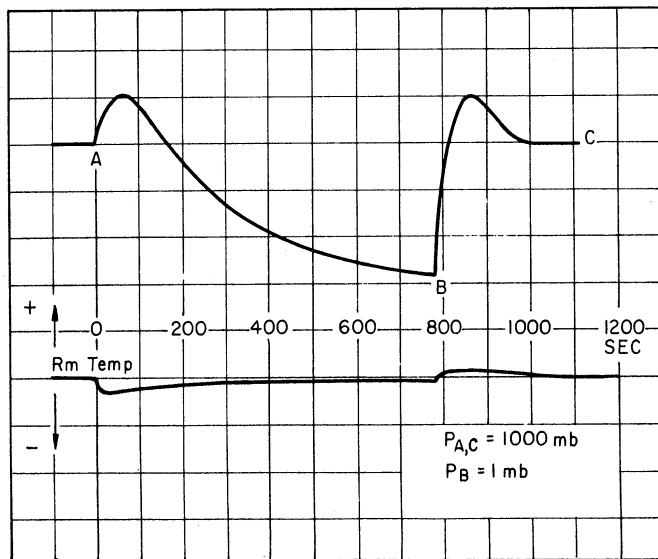
During one series of tests, both collected current and gas temperature, as measured by a thermistor of very low mass, were recorded. The observed adiabatic temperature changes under conditions of rapid pressure change were compared with the corresponding chamber currents for correlation which was readily apparent. The amount of the change in temperature (typical Δt of 30°-40°C) was found as expected to be proportional to the volume of the gage, the gas pressure, and the rate of change in pressure. The output current was found to respond to these changes in temperature so that the maximum of the i-p characteristic became higher during pumping out (drop in temperature), and vice versa. It was possible to reduce or almost eliminate the difference between the peak values by lowering the pumping speed as illustrated in Fig. 14. Considering these effects and the concept that a gage characteristic plotted as current vs. density should be independent of temperature insofar as the gas law



Case (a). Full Pumping Speed



Case (b). 1/2 Full Speed



Case (c). 1/10 Full Speed

Fig. 14. Change of output current and "gas" temperature with time for various pumping speeds.

is concerned, it seems probable that hysteresis is most likely due to variation with temperature of the attachment and recombination coefficients. With this in mind, changes in gage design to increase the surface-to-volume ratio were made to improve the effective accommodation coefficient at the higher densities. Gages constructed thusly exhibited markedly less hysteresis, substantiating the above reasoning. Additional similar tests were conducted considering the apparent importance of the area-to-volume ratio, further validating the explanation.

CONCLUDING REMARKS

The foregoing describes the work carried out under this contract in investigation of the properties of a radioactive ionization gage. Although the conclusion that hysteresis is caused by temperature dependence of the attachment and recombination coefficients should be more firmly established by further testing and study, this somewhat incomplete investigation has resulted in a new gage design largely eliminating this effect.

Further improvements of the chamber from the standpoint of sensitivity, size, and radioactive hazard have been made in connection with application of the chamber to upper-atmosphere measurements. Redesign of the associated electronic circuitry has likewise been accomplished in conjunction with application to upper-atmosphere measurements, and is discussed in a report pertaining to that effort. Thus this report partially fulfills the obligations of the contract.

APPENDIX

ANALYTICAL INVESTIGATION OF SOURCE STABILITY

The disintegration of radium and its decay products results in the emission of alpha, beta, and gamma rays which, in their passage through gases, produce ionization. The specific ionization varies greatly for the three products, roughly in the ratio 10,000 : 100 : 1, respectively. We need, therefore, concern ourselves with the alpha particles only.

The successive transformations of radium and its decay products are illustrated in Fig. 15 which shows the type and range, in standard air, of particles emitted, as well as the half-life time of the successive elements. All the decay products of radium (Ra) are solid substances except radon (Rn) which is gaseous under normal conditions.

CASE I

Since the half-life time of disintegration of radium is considerably long (1200 years), it is perfectly justifiable to assume that, for an interval of a few days, the disintegration of radium (Ra) takes place at a constant rate, n_0 particles per second. This also means that radon gas is emanating from radium at the same rate, n_0 particles per second.

It is known that the rate of disintegration of any radioactive material depends on the amount as well as the kind of material. This could be expressed as

$$\frac{dN}{dt} = -\lambda N ,$$

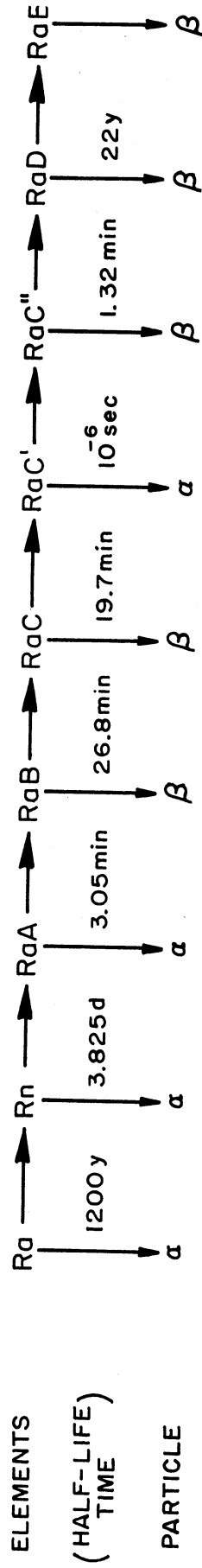
where N is the number of particles at any instant, t , and λ is a characteristic constant of each element independent of all physical and chemical conditions.

The net change of radon (dp) in an interval dt is then given by

$$dp = (n_0 - \lambda_1 p) dt ,$$

or

$$\frac{dp}{dt} + \lambda_1 p = n_0 ,$$



RANGE (cms)

3.389

4.1

4.7

6.97

Fig. 15. Radioactive transformation of radium and its decay products.

where p is the amount of radon present at any instant and λ_1 is the characteristic constant for the same material. Assuming radon was initially absent, then p is given by

$$p = \frac{n_0}{\lambda_1} (1 - e^{-\lambda_1 t}) .$$

Similarly for Ra A

$$\frac{dq}{dt} = \lambda_1 p - \lambda_2 q ,$$

where q is the amount of Ra A at any instant and λ_2 is the characteristic constant of Ra A.

Substituting for p and transposing, we get

$$\frac{dq}{dt} + \lambda_2 q = n_0 (1 - e^{-\lambda_1 t}) .$$

Considering Ra A initially absent, then the solution for q is

$$q = \frac{n_0}{\lambda_2} - \frac{n_0}{\lambda_2 - \lambda_1} e^{-\lambda_1 t} - \frac{n_0 \lambda_1}{\lambda_2 (\lambda_1 - \lambda_2)} e^{-\lambda_2 t} .$$

In the same way the values of Ra B and Ra C are, respectively,

$$r = \frac{n_0}{\lambda_3} - \frac{n_0 \lambda_2}{(\lambda_2 - \lambda_1)(\lambda_3 - \lambda_1)} e^{-\lambda_1 t} - \frac{n_0 \lambda_1}{(\lambda_1 - \lambda_2)(\lambda_3 - \lambda_2)} e^{-\lambda_2 t} - \frac{n_0 \lambda_1 \lambda_2}{\lambda_3 (\lambda_1 - \lambda_3)(\lambda_2 - \lambda_3)} e^{-\lambda_3 t}$$

and

$$s = \frac{n_0}{\lambda_4} - \frac{n_0 \lambda_2 \lambda_3}{(\lambda_2 - \lambda_1)(\lambda_3 - \lambda_1)(\lambda_4 - \lambda_1)} e^{-\lambda_1 t} - \frac{n_0 \lambda_1 \lambda_3}{(\lambda_1 - \lambda_2)(\lambda_3 - \lambda_2)(\lambda_4 - \lambda_2)} e^{-\lambda_2 t}$$

Since the half-life time of Ra C is very small, 10^{-6} seconds, no further calculations are needed beyond Ra C to cater for the fourth alpha particle. Therefore, the build-up of the alpha activity $N(t)$ of the sealed source becomes

$$N(t) = n_0 + \lambda_1 p + \lambda_2 q + \lambda_4 s \quad \text{alpha/sec}$$

or

$$N(t) = n_0 [4 - a_1 e^{-\lambda_1 t} - a_2 e^{-\lambda_2 t} - a_3 e^{-\lambda_3 t} - a_4 e^{-\lambda_4 t}] ,$$

where

$$a_1 = 1 + \frac{\lambda_2}{\lambda_2 - \lambda_1} + \frac{\lambda_2 \lambda_3 \lambda_4}{(\lambda_2 - \lambda_1)(\lambda_3 - \lambda_1)(\lambda_4 - \lambda_1)},$$

$$a_2 = \frac{\lambda_1}{\lambda_1 - \lambda_2} + \frac{\lambda_1 \lambda_3 \lambda_4}{(\lambda_1 - \lambda_2)(\lambda_3 - \lambda_2)(\lambda_4 - \lambda_2)},$$

$$a_3 = \frac{\lambda_1 \lambda_2 \lambda_4}{(\lambda_1 - \lambda_3)(\lambda_2 - \lambda_3)(\lambda_4 - \lambda_3)}, \text{ and}$$

$$a_4 = \frac{\lambda_1 \lambda_2 \lambda_3}{(\lambda_1 - \lambda_4)(\lambda_2 - \lambda_4)(\lambda_3 - \lambda_4)}.$$

At the steady state,

$$n_0 = \lambda_1 P_0 = \lambda_2 Q_0 = \lambda_3 R_0 = \lambda_4 S_0,$$

where P_0 , Q_0 , R_0 , and S_0 are the equilibrium contents of radon, Ra A, Ra B, and Ra C, respectively.

CASE II

In this case it is considered that the source is not perfectly sealed under vacuum; consequently the alpha activity will be partially affected as a result of the continuous loss in the active radon. The source, however, is assumed to be well sealed under atmospheric pressure. Because of the loss in radon through the seal, the rate of supply of radon is taken as $n_0 e^{-\alpha t}$, where α is a constant, for mathematical simplicity, and $\alpha < \lambda_1$.

The source activity, in this case, undergoes two different changes: (a) during the pumping out period the activity is continuously affected by loss of part of the radon generated, and (b) under atmospheric pressure no further losses are assumed and the source starts to increase activity.

To summarize the procedure carried out in Case II: (i) one starts with a source under equilibrium, i.e., with

$$P_0 = \frac{n_0}{\lambda_1}, \quad Q_0 = \frac{n_0}{\lambda_2}, \quad R_0 = \frac{n_0}{\lambda_3}, \quad \text{and} \quad S_0 = \frac{n_0}{\lambda_4},$$

as the initial contents of Rn, Ra A, Ra B, and Ra C, respectively; (ii) the source is then kept under vacuum for an interval of time T , at the end of which the radioactive contents, as a result of radon loss, will have the values P_T , Q_T , R_T , and S_T , respectively; (iii) radon loss is then assumed to stop after exposing and keeping the source under atmospheric pressure for a long period

during which it builds up its activity with P_T , Q_T , R_T , and S_T as the new initial contents.

To find p , q , r , and s under vacuum, one follows the same procedure used in Case I with P_0 , Q_0 , R_0 , S_0 , the equilibrium contents, as initial values for radon, Ra A, Ra B, and Ra C, respectively, and $n_0 e^{-\alpha t}$ instead of n_0 as the rate of production of radon. Then the instantaneous values of radon, Ra A, Ra B, Ra C, respectively, are:

$$p(t) = \frac{n_0}{\lambda_1 - \alpha} e^{-\alpha t} + N e^{-\lambda_1 t},$$

$$q(t) = \frac{n_0 \lambda_1}{(\lambda_1 - \alpha)(\lambda_2 - \alpha)} e^{-\alpha t} + \frac{\lambda_1 N}{\lambda_2 - \lambda_1} e^{-\lambda_1 t} + A e^{-\lambda_2 t},$$

$$r(t) = \frac{n_0 \lambda_1 \lambda_2}{(\lambda_1 - \alpha)(\lambda_2 - \alpha)(\lambda_3 - \alpha)} e^{-\alpha t} + \frac{\lambda_1 \lambda_2 N}{(\lambda_2 - \lambda_1)(\lambda_3 - \lambda_1)} e^{-\lambda_1 t} + \frac{\lambda_2 A}{\lambda_3 - \lambda_2} e^{-\lambda_2 t} + B e^{-\lambda_3 t},$$

and

$$s(t) = \frac{n_0 \lambda_1 \lambda_2 \lambda_3}{(\lambda_1 - \alpha)(\lambda_2 - \alpha)(\lambda_3 - \alpha)(\lambda_4 - \alpha)} e^{-\alpha t} + \frac{\lambda_1 \lambda_2 \lambda_3 N}{(\lambda_2 - \lambda_1)(\lambda_3 - \lambda_1)(\lambda_4 - \lambda_1)} e^{-\lambda_1 t} \\ + \frac{\lambda_2 \lambda_3 A}{(\lambda_3 - \lambda_2)(\lambda_4 - \lambda_2)} e^{-\lambda_2 t} + \frac{\lambda_3 B}{(\lambda_4 - \lambda_3)} e^{-\lambda_3 t} + C e^{-\lambda_4 t},$$

where

$$N = \frac{n_0}{\lambda_1} - \frac{n_0}{\lambda_1 - \alpha},$$

$$A = \frac{n_0}{\lambda_2} - \frac{\lambda_1 N}{\lambda_2 - \lambda_1} - \frac{n_0 \lambda_1}{(\lambda_1 - \alpha)(\lambda_2 - \alpha)},$$

$$B = \frac{n_0}{\lambda_3} - \frac{\lambda_2 A}{\lambda_3 - \lambda_2} - \frac{\lambda_1 \lambda_2 N}{(\lambda_3 - \lambda_1)(\lambda_2 - \lambda_1)} - \frac{n_0 \lambda_1 \lambda_2}{(\lambda_1 - \alpha)(\lambda_2 - \alpha)(\lambda_3 - \alpha)}, \text{ and}$$

$$C = \frac{n_0}{\lambda_4} - \frac{\lambda_3 B}{\lambda_4 - \lambda_3} - \frac{\lambda_2 \lambda_3 A}{(\lambda_3 - \lambda_2)(\lambda_4 - \lambda_2)} - \frac{\lambda_1 \lambda_2 \lambda_3 N}{(\lambda_2 - \lambda_1)(\lambda_3 - \lambda_1)(\lambda_4 - \lambda_1)} - \frac{\lambda_1 \lambda_2 \lambda_3 n_0}{(\lambda_1 - \alpha)(\lambda_2 - \alpha)(\lambda_3 - \alpha)(\lambda_4 - \alpha)}.$$

P_T , Q_T , R_T , and S_T could then be calculated by substituting T for t .

Now, on raising the pressure to atmospheric and assuming no further loss of radon under these conditions, the activity of the source as an alpha emitter could be evaluated by following exactly the same lines as before. In this case the total activity is given by the sum of the activity in Case I and that of

radon, Ra A, Ra B, and Ra C with P_T , Q_T , R_T , and S_T as initial amounts, respectively.

Then the activity of the source becomes:

$$N'(t) = 4 n_0 - a_1(n_0 - \lambda_1)P_T e^{-\lambda_1 t} - \left[n_0 a_2 - \lambda_2 Q' - \frac{\lambda_2 \lambda_3 \lambda_4 Q'}{(\lambda_3 - \lambda_2)(\lambda_4 - \lambda_2)} \right] e^{-\lambda_2 t} \\ - \left[n_0 a_3 - \frac{\lambda_3 \lambda_4 R'}{\lambda_4 - \lambda_3} \right] e^{-\lambda_3 t} - [n_0 a_4 - \lambda_4 S'] e^{-\lambda_4 t} ,$$

where a_1, a_2, a_3, a_4 are the same as in Case I,

$$Q' = Q_T - \frac{\lambda_1}{\lambda_2 - \lambda_1} P_T ,$$

$$R' = R_T - \frac{\lambda_2}{\lambda_3 - \lambda_2} Q' - \frac{\lambda_1 \lambda_2}{(\lambda_3 - \lambda_1)(\lambda_2 - \lambda_1)} P_T , \text{ and}$$

$$S' = S_T - \frac{\lambda_3 R'}{\lambda_4 - \lambda_3} - \frac{\lambda_2 \lambda_3 Q'}{(\lambda_3 - \lambda_2)(\lambda_4 - \lambda_2)} - \frac{\lambda_1 \lambda_2 \lambda_3 P_T}{(\lambda_4 - \lambda_1)(\lambda_3 - \lambda_1)(\lambda_2 - \lambda_1)} .$$

The result of some numerical examples is shown in Fig. 9, where three cases were considered.

(A) $T = 72$ hours,

(B) $T = 72$ hours,

(C) $T = 240$ hours.

The values of $\lambda_1, \lambda_2, \lambda_3,$ and λ_4 are the conventional values for radon, Ra A, Ra B, and Ra C, respectively.

UNIVERSITY OF MICHIGAN



3 9015 02827 4416